

**IDEAL, INERT AND REACTIVE HYPERSONIC FLOW SIMULATIONS OVER
BLUNT BODY****Carlos Alberto Rocha Pimentel**UNIVAP - Universidade do Vale do Paraíba
São José dos Campos - SP - 12244-000 - Brazil
cearapim@univap.br**Heidi Korzenowski**UNIVAP - Universidade do Vale do Paraíba
São José dos Campos - SP - 12244-000 - Brazil
heidi@univap.br

Abstract. *The present work performs an inviscid hypersonic flow simulations over a re-entry body. A small ballistic re-entry vehicle SARA configuration is numerically investigated by using the Euler equations. The governing equations are discretized in conservative form in a cell centered, finite volume procedure for unstructured triangular grids. Spatial discretization considers a second-order van Leer scheme. A MUSCL reconstruction of primitive variables is used in order to determine left and right states at interfaces. An adaptive mesh refinement procedure was used in order to conduct the ideal gas numerical simulations. Time march uses, an explicit 2nd-order accurate, 5-stage Runge-Kutta time stepping scheme. 79% of Nitrogen and 21% of Oxygen composes the gas. The Gardiner chemical kinetics considers 5 species (N_2 , O_2 , O , N , NO), with their combination and dissociation reactions. Mach number and pressure contours will be presented. Ideal, inert and real gas will be considered. The simulations are performed considering freestream Mach number 7.*

Keywords: *hypersonic flow simulation, finite volume, unstructured grids.*

1. Introduction

The development of efficient numerical solvers is very important owing to the difficulties and high costs associated with the experimental work at high speed flows. Typical hypersonic flows undergo chemical and thermal processes that are very difficult to predict experimentally. Hence, the numerical simulation plays an important role in hypersonic vehicle design. The focus of the numerical methods is on the accurate simulation of flows with strong shock waves, capturing complex flow phenomena and variations in the variables for hypersonic flows.

The hypersonic fluid flow simulation over a re-entry body is quite some interesting in sense that a strong detached normal shock wave in the nose region is generated. This phenomenon is particularly interesting because the curved bow shock is a normal shock wave in the nose region, and away from this one has all possible oblique shock solutions for a given freestream Mach number.

A finite volume formulation of compressible Euler equations in conservative form has been considered. A high-resolution scheme is employed in order to obtain a good spatially resolution of the flow features. In this work the simulations are performed by using a second-order van Leer flux-vector splitting scheme, implemented in an unstructured grid context (Azevedo and Korzenowski, 1998). This scheme considers a MUSCL approach (Hirsh, 1990), that is, the interface fluxes are formed using left and right states at the interface, which are linearly reconstructed by primitive variable extrapolation on each side of the interface. A minmod limiter (Hirsh, 1990) is used in order to avoid any undesired oscillations in the solution. The equations are discretized in a cell centered based finite volume procedure on triangular meshes. Time march uses an explicit, second-order accurate, five-stage Runge-Kutta time stepping scheme.

For the gas flow simulations one considers that 79% of Nitrogen and 21% of Oxygen composes the gas. Real gas effects are considered for the reactive flow simulations (Pimentel, 2000). The chemical kinetic mechanism considers five chemical species, with their combination and dissociation reactions. The computations are performed considering $M_\infty = 7$. Results obtained for the inviscid simulations are presented, in order to analyse the phenomena presented in such flows. Results indicate that the scheme could adequately capture the flowfield features.

The ideal gas flow simulation is concerned with the implementation of unstructured grid, mesh refinement techniques for two-dimensional inviscid flow problems of aerospace interest. The mesh refinement procedure

uses a numerical sensor based on flow physical properties. The present development should be seen as an evolutionary step towards the desired three-dimensional capability. The goal is to develop all the criteria necessary to construct adaptive meshes suitable to the desired applications in the 2-D case, for computational cost reasons.

2. Mathematical Model for Numerical Simulations

The two-dimensional time-dependent, compressible Euler equation may be described, in conservative vector form, by

$$\frac{\partial Q}{\partial t} + \frac{\partial E}{\partial x} + \frac{\partial F}{\partial y} = 0, \quad (1)$$

where the vectors E e F are conservative flux vectors, and Q is the vector of conservative quantities. If the equations are discretized in a cell centered finite volume procedure, the discrete vector of conserved variables, Q_i , is defined as an average over the i_{th} control volume. In this context, the flow variables can be assumed as attributed to the centroid of each cell. The Eq. (1) can be written in integral form for the i_{th} control volume as

$$\frac{\partial}{\partial t}(V_i Q_i) + \int_S (E dy - F dx) = 0 \quad (2)$$

V represents the area of the control volume and S its boundary.

The supersonic reactive flow will be computed using the unsteady 2-D Euler equations (Pimentel, 2000), thus neglecting molecular transport. These balance equations of mass, momentum, energy and species mass fraction can be written as

$$\frac{\partial Q}{\partial t} + \frac{\partial E}{\partial x} + \frac{\partial F}{\partial y} = \Omega, \quad (3)$$

where

$$Q = [\rho, \rho u, \rho v, \rho \mathcal{E}, \rho Y_1, \dots, \rho Y_{K-1}]^T, \quad E = \begin{bmatrix} \rho u \\ \rho u^2 + p \\ \rho uv \\ u(\rho \mathcal{E} + p) \\ \rho Y_1 u \\ \vdots \\ \rho Y_{K-1} u \end{bmatrix}, \quad F = \begin{bmatrix} \rho v \\ \rho uv \\ \rho v^2 + p \\ v(\rho \mathcal{E} + p) \\ \rho Y_1 v \\ \vdots \\ \rho Y_{K-1} v \end{bmatrix}, \quad (4)$$

and

$$\Omega = [0, 0, 0, 0, \dot{\omega}_1 W_1, \dots, \dot{\omega}_{K-1} W_{K-1}]^T, \quad (5)$$

with p , Y_K and \mathcal{E} given by

$$Y_K = 1 - \sum_{k=1}^{K-1} Y_k, \quad p = \rho R T \sum_{k=1}^K \frac{Y_k}{W_k}, \quad \mathcal{E} = e + \frac{1}{2}(u^2 + v^2) = \sum_{k=1}^K Y_k e_k + \frac{1}{2}(u^2 + v^2), \quad (6)$$

where

$$e_k = h_k^0 + \int_{T_0}^T c_{p_k} dT - \frac{p}{\rho}. \quad (7)$$

In these equations \mathcal{E} is the total energy per unit of mass, e is the internal energy, R is the universal gas constant. The internal energy, the standard-state enthalpy and the specific heat at constant pressure per unit of mass of species k are noted e_k , h_k^0 and c_{p_k} . Y_k , $\dot{\omega}_k$ and W_k are the mass fraction, the molar production rate and the molecular weight of chemical species k , respectively.

3. Chemical Kinetics Mechanism

The chemical kinetics mechanism for the reactive mixture of nitrogen and oxygen is due to Gardiner (Hachemin, 1995). This mechanism considers 5 species (N_2 , O_2 , N , O , NO) and 21 elementary reactions, and is given in Tab. (1).

The chemical production rates are given by the Arrhenius law :

$$k_f = AT^\beta \exp(-E/RT). \quad (8)$$

The calculation of k_f and of the molar production rates $\dot{\omega}_k$ are performed using the CHEMKIN-II package (Hachemin, 1995). The thermodynamic properties are calculated according to the procedures developed by Kee *et al*, 1991.

Table 1: Reaction mechanism for N_2 - O_2 : A in (cm,mol,s), E in (Kelvins).

Reactions	A	β	E
$N_2 + N_2 \rightarrow 2N + N_2$	3.7e21	-1.6	113200.
$2N + N_2 \rightarrow N_2 + N_2$	1.08e13	-1.493	100.
$N_2 + O_2 \rightarrow 2N + O_2$	1.4e21	-1.6	113200.
$2N + O_2 \rightarrow N_2 + O_2$	3.07e13	-1.493	100.
$N_2 + NO \rightarrow 2N + NO$	1.4e21	-1.6	113200.
$2N + NO \rightarrow N_2 + NO$	3.07e13	-1.493	100.
$N_2 + N \rightarrow 2N + N$	1.6e22	-1.6	113200.
$2N + N \rightarrow N_2 + N$	3.51e14	-1.493	100.
$N_2 + O \rightarrow 2N + O$	1.4e21	-1.6	113200.
$2N + O \rightarrow N_2 + O$	3.07e13	-1.493	100.
$O + O + M \rightarrow O_2 + M$	3.64e18	-1.0	59380.
$2O + N_2 \rightarrow O_2 + N_2$	1.84e10	-0.714	109.
$O_2 + O_2 \rightarrow 2O + O_2$	1.64e19	-1.0	59380.
$2O + O_2 \rightarrow O_2 + O_2$	8.28e10	-0.714	109.
$O_2 + NO \rightarrow 2O + NO$	1.82e18	-1.0	59380.
$2O + NO \rightarrow O_2 + NO$	9.19e09	-0.714	109.
$O_2 + N \rightarrow 2O + N$	1.82e18	-1.0	59380.
$2O + N \rightarrow O_2 + N$	9.19E09	-0.714	109.
$O_2 + O \rightarrow 2O + O$	4.56e19	-1.0	59380.
$2O + O \rightarrow O_2 + O$	2.3e11	-0.714	109.
$NO + N_2 \rightarrow N + O + N_2$	4.0e20	-1.5	75500.
$N + O + N_2 \rightarrow NO + N_2$	2.16e19	-1.3217	97.
$NO + O_2 \rightarrow N + O + O_2$	4.0e20	-1.5	75500.
$N + O + O_2 \rightarrow NO + O_2$	2.16e19	-1.3217	97.
$NO + NO \rightarrow N + O + NO$	8.0e20	-1.5	75500.
$N + O + NO \rightarrow NO + NO$	4.32e19	-1.3217	97.
$NO + N \rightarrow N + O + N$	8.0e20	-1.5	75500.
$N + O + N \rightarrow NO + N$	4.32e19	-1.3217	97.
$NO + O \rightarrow N + O + O$	8.0e20	-1.5	75500.
$N + O + O \rightarrow NO + O$	4.32e19	-1.3217	97.
$N_2 + O \rightarrow NO + N$	1.82e14	0.0	38370.
$NO + N \rightarrow N_2 + O$	7.35e13	-0.07083	666.
$NO + O \rightarrow O_2 + N$	3.8e09	1.0	20820.
$O_2 + N \rightarrow NO + O$	4.07e10	0.886	4689.

4. Spatial Discretization Algorithm

The implementation of the 2nd-order scheme is based on an extension of the Godunov approach. The projection stage of the Godunov scheme, in which the solution is projected in each cell on piecewise constant states, is modified. This constitutes the so-called MUSCL approach for the extrapolation of primitive variables (van Leer, 1995). By this approach, left and right states at a given interface are linearly reconstructed by primitive variable extrapolation on each side of the interface, together with some appropriate limiting process in order to avoid the generation of new extrema.

The convective operator, $C(Q_i)$, which discretize the surface integral of Eq. (2), is defined for the van Leer flux vector splitting scheme by the expression

$$C(Q_i) = \sum_{k=1}^3 (E_{ik} \Delta y_{ik} - F_{ik} \Delta x_{ik}) . \quad (9)$$

The interface fluxes, E_{ik} and F_{ik} , are defined as

$$\begin{aligned} E_{ik} &= E^+(Q_L) + E^-(Q_R) , \\ F_{ik} &= F^+(Q_L) + F^-(Q_R) . \end{aligned} \quad (10)$$

where Q_L and Q_R are the left and right states at the ik interface obtained by linear extrapolation process.

5. Results and Discussion

The simulations were performed over the small ballistic re-entry vehicle SARA configuration, considering $M_\infty = 7$. The adaptive mesh adopted in the present inviscid flow simulations, considering ideal gas, was obtained with two passes of refinement. These refined levels were performed when the L_2 norm of change in density variable drops two order of magnitude. Typically, around 2500 iterations are required to satisfy this convergence criterion. The sensor was based on all primitive variable gradients. No freezing of limiters was used here. The initial mesh has 3036 nodes and 5890 volumes, while the adaptive mesh is composed of 5072 nodes and 9232 volumes. The initial and final meshes for inviscid flow numerical simulations, ideal gas, are shown in the Figure (1).

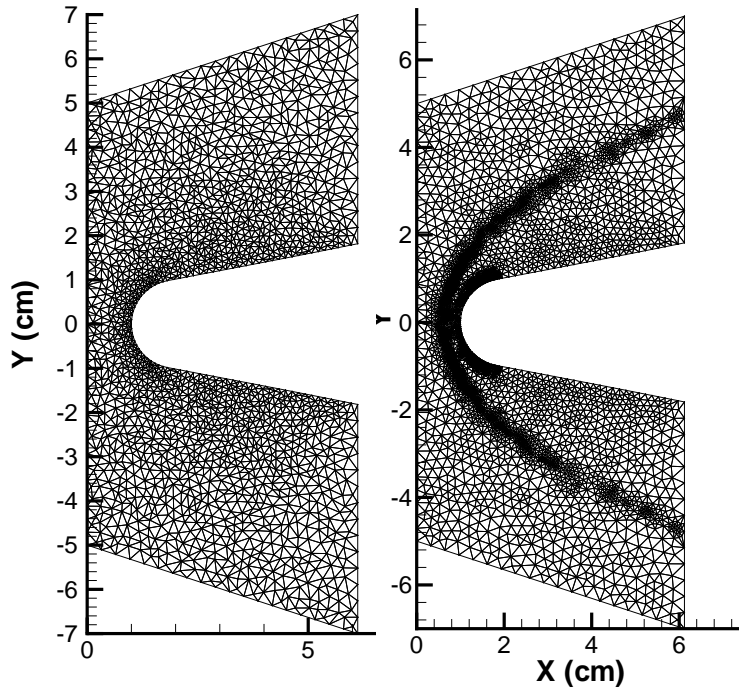


Figure 1: Initial and adaptive mesh used considering ideal gas flow simulations.

The temperature contours obtained with the second-order van Leer flux vector splitting scheme, with ideal gas assumption, are presented in Figure (1). Initial conditions for this simulation consider that all properties were dimensionless.

The contours indicate that the flow features are well captured by this solution, the bow shock and the flow expansion over the body are well represented. The shock at the nose of the body is a normal shock, and away from this the shock wave gradually becomes curved and weaker. The hypersonic flow ahead the normal shock becomes subsonic, that is, there is a strong compression of the flow in this region. Slightly above the nose region, the shock is oblique and pertains to the strong shock-wave solution. As one move further along the shock, the

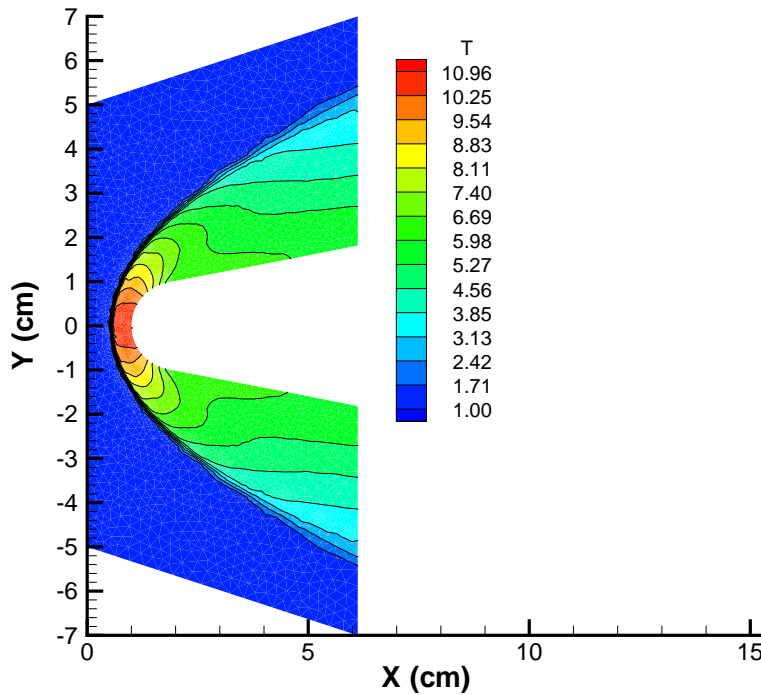


Figure 2: Temperature contours considering ideal gas simulation.

wave angle becomes more oblique, and the flow deflection decreases until reach the maximum deflection angle. From the nose region until this point the flow is subsonic, and above it, all points on the shock correspond to the weak shock solution, and the region is characterized by supersonic flow.

The pressure, density and temperature properties, downstream of the wave, obtained by use of the basic normal shock equations, are $p_2/p_1 = 57$, $\rho_2/\rho_1 = 5.444$, $T_2/T_1 = 10.47$, respectively. The properties obtained by the numerical solution simulations are $p_2/p_1 = 58.31$, $\rho_2/\rho_1 = 5.6073$, $T_2/T_1 = 10.83$. One can observe a maximum error of 3.5 % between the analytical and numerical results, indicating that the scheme was adequate to assess the properties of the flow.

The Figure (2) shows the temperature contours obtained with freestream Mach number 7. Initial conditions for these simulations were set as pressure of 0.1848 atm and temperature of 300 K. In this case, inert gas assumption was adopted. This result was obtained by using an axysymmetric formulation, with van Leer 2nd-order splitting scheme. The mesh used in this case has 9292 nodes and 17999 volumes. No adaptive refinement procedure was used in these simulations.

One can observe that the temperature contours are well captured by this numerical method, the shock and the stagnation region are well represented. The streamline that passes through this normal portion of the shock impinges on the nose of the body and controls the values of stagnation pressure and temperature at the nose.

The same initial conditions and the same mesh used for the inert gas flow simulations were used to perform the reactive gas flow simulations. The temperature contours obtained considering real gas effects are presented in Figure (3), for $M_\infty = 7$.

The pressure results obtained with the inert (24.45 atm) and the pressure obtained with chemical reactions flow simulations (22 atm) can show that, if one considers real gas effects, the stagnation properties would decay due the formation of species dissociation. The Tab. (2) presents the and the temperature values downstream the shock wave and the results in the stagnation region. For the stagnation region one considers $y = 0.1$ cm and $x = 2.45$ cm, and after the shock wave one considers $y = 0.1$ cm and $x = 2.2$ cm.

One can observe a good agreement between theoretical and numerical values. For the pressure after the shock wave, the difference between these approaches is 10.35%. But, if one observe the temperature results, one can verify that the difference between inert and reactive gas simulations results is 0.04%. The small Mach number promotes the small difference between inert and reactive gas simulations.

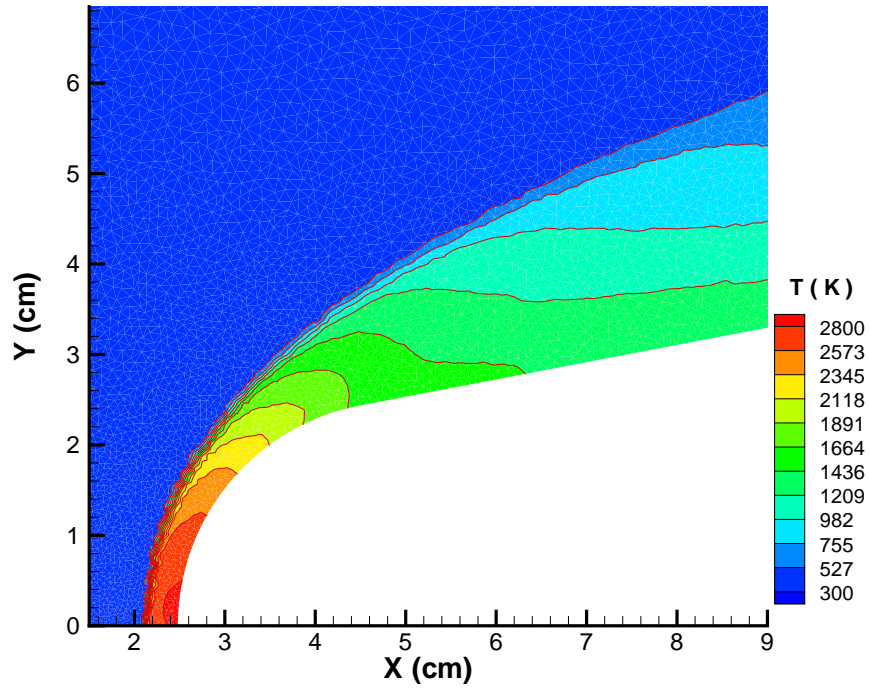


Figure 3: Temperature contours considering inert gas simulation.

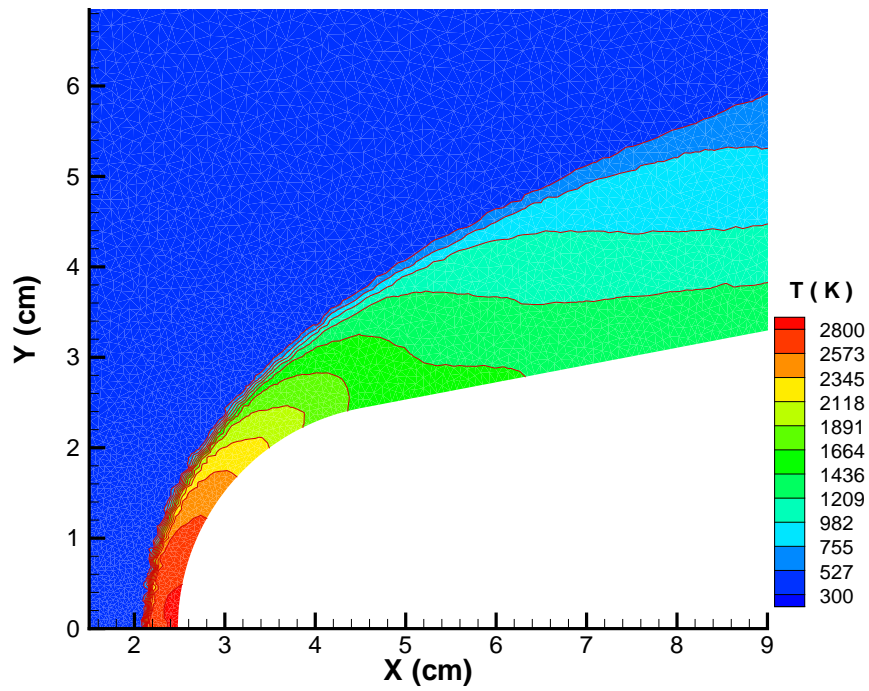


Figure 4: Temperature contours considering real gas effects, temperature in K.

Table 2: Pressure and temperature downstream the shock wave and in the stagnation region.

	theoretical	inert simulations	reactive gas simulations
p_2 (atm)	10.43	9.34943	9.34506
T_2 (K)	2937.78	2731.6	2730.64
p_{t2} (atm)	11.55	10.893	10.8912
T_{t2} (K)	3019.5	2819.82	2811.47

6. Conclusions

The present work performed an inviscid hypersonic flow simulation over a blunt body. Ideal, inert and chemical reaction flow simulations were performed. 79% of Nitrogen and 21% of Oxygen composes the gas. For the chemical reaction flow simulations, five chemical species were considered, with their combination and dissociation. The governing equations were discretized in an unstructured triangular mesh by a cell centered finite volume algorithm. The equations were advanced in time by an explicit, 5-stage, 2nd-order accurate, Runge-Kutta time stepping procedure. The spatial discretization considered a 2nd-order van Leer flux-vector splitting scheme. A MUSCL reconstruction of primitive variables was performed in order to obtain left and right states at interfaces.

7. Acknowledgments

The first author gratefully acknowledge the support of CAPES (Coordenação de Aperfeiçoamento de Pessoal de Nível Superior) - Brazil, while he was a graduate student with a scholarship. The second author acknowledge the support of FAPESP under the Project Research Grant No. 98/09812-6. The authors wishes to thank the Brazilian Space Agency under financial support.

8. References

- Azevedo, J.L.F., Figueira da Silva, L.F., 1997, "The Development of an Unstructured Grid Solver for Reactive Compressible Flow Applications," AIAA Paper 97-3239, 33rd AIAA/ASME/SAE/ASEE Joint Propulsion Conference & Exhibit, Seattle, WA.
- Azevedo, J.L.F., Korzenowski, H., 1998, "Comparison of Unstructured Grid Finite Volume Methods for Cold Gas Hypersonic Flow Simulations," AIAA Paper 98-2629, 16th AIAA Applied Aerodynamics Conference, Albuquerque, USA.
- Drikakis, D., Tsangaris, S., 1993, "On the Accuracy and Efficiency of CFD Methods in Real Gas Hypersonics," International Journal for Numerical Methods in Fluids, Vol. 16, 759-775.
- Hachemin, Jean-Victor, 1995, "Developpement d'un code Navier-Stokes parabolise pour des ecoulements tridimensionnels en desequilibre thermochimique," Note Technique 1995-8, FR ISSN 0078-3781, France.
- Hirsch, C., 1990, "Numerical Computation of Internal and External Flows. Vol. 2: Computational Methods for Inviscid and Viscous Flows", Wiley, New York.
- Kee, R.J., Rupley, F.M., and Miller, J.A., 1991, CHEMKIN-II: A fortran chemical kinetics package for the analysis of gas phase chemical kinetics, Sandia National Laboratories Technical Rep. SAND86-8009B/UC-706.
- Korzenowski, H., Maciel, E.S.G., and Azevedo, J.L.F., 1998, "Adaptive Mesh Refinement on the Solution of Two-Dimensional Viscous Aerospace Problems," ICAS Paper No. 98-2.2.3, Proceedings of the 21st Congress of the International Council of the Aeronautical Sciences, Melbourne, Australia.
- Pimentel, C. A. R., 2000, "Etude Numerique de La Transition entre Une Onde de Choc Oblique Stabilisee Par Un Diedre et Une Onde de Detonation Oblique", Thèse Doctorale, Université de Poitiers.
- van Leer, B., 1995, "Flux-vector Splitting for the Euler Equations" Proceedings of the 8th International Conference Numerical Methods in Fluid Dynamics, E. Krause, editor, Lecture Notes in Physics, vol. 170, pp. 507-512.